Bone 143 (2021) 115754

Contents lists available at ScienceDirect

Bone

journal homepage: www.elsevier.com/locate/bone

Osteoblastic Wnt1 regulates periosteal bone formation in adult mice

Fan Wang [a], Petri Rummukainen [a], Terhi J. Heino [a], Riku Kiviranta [a,b,*]

[a] Institute of Biomedicine, University of Turku, Turku, Finland
[b] Department of Endocrinology, Division of Medicine, University of Turku and Turku University Hospital, Turku, Finland

ARTICLE INFO

Keywords:
Wnt1
Osteoblast
Cortical bone thickness
Periosteal bone
Modeling-based bone formation

ABSTRACT

Compelling clinical data together with genetically modified mouse models have demonstrated that Wnt1 is a key Wnt ligand in bone metabolism, regulating both osteoblast activity and osteoclast differentiation. We have previously shown that deletion of Wnt1 in limb mesenchymal cells leads to severe ostepenic bone phenotype and spontaneous fractures very early after birth. However, the function of Wnt1 in mature skeleton remained unknown. To investigate the role of Wnt1 specifically in adult bone metabolism, we generated an osteoblast lineage-targeted inducible Wnt1 knockout mouse model using tetracycline-controlled Osterix-Cre mouse line (Osx-Cre). In this model, the Cre recombinase expression is suppressed by administering doxycycline (Dox) in drinking water. As expected, $Wnt1^{-/-}_{Osx}$ mice without Dox developed spontaneous fractures early by 3 weeks of age due to severe trabecular and cortical osteopenia. Administration of Dox to $Wnt1^{-/-}_{Osx\text{-}Dox}$ and control mice until 4 weeks of age suppressed Wnt1 deletion and completely prevented the fractures. Withdrawal of Dox led to deletion in Wnt1 allele but the fracture incidence progressively decreased in $Wnt1^{-/-}_{Osx\text{-}Dox}$ mice at 8 or 12 weeks of age (4 and 8 weeks after Dox withdrawal). Interestingly, deletion of Wnt1 at 4 weeks of age resulted only in a modest and transient trabecular osteopenia that was more pronounced in females and was normalized by 12 weeks of age. However, diaphyseal cortical bone mass and cortical thickness in the femurs were significantly decreased in $Wnt1^{-/-}_{Osx\text{-}Dox}$ mice of both genders. Mechanisticly, this was due to impaired periosteal bone formation. Based on our data, in addition to its essential role in early skeletal growth, Wnt1 is an important regulator of modeling-based bone formation and cortical thickness in adult mice.

1. Introduction

Osteoporosis is a progressive systemic skeletal disease characterized by low bone mass, microarchitectural deterioration of bone structure and increased bone porosity, resulting in bone fragility and susceptibility to fractures [1–3]. Numerous human genetic studies and genetically modified mouse models have demonstrated that Wnt signaling pathway plays essential roles in the regulation of bone formation and resorption [4]. We and others discovered that *WNT1* mutations in patients cause early-onset osteoporosis and osteogenesis imperfecta (OI) [5–8]. A homozygous *WNT3* mutation in human causes Tetra-Amelia syndrome, which is characterized by the absence of all four limbs [9], while mutations in *WNT7A* cause a range of limb malformations, including Fuhrmann syndrome and Al-Awadi/Raas-Rothschild and Schinzel phocomelia syndromes [10–13]. Furthermore, non-canonical Wnt signaling pathway has also been linked to skeletal development. Osteoblast lineage cell-derived Wnt5a enhances osteoclastogenesis through Wnt5a-Ror2 signaling pathway [14,15], while osteoblast-derived Wnt16 prevents cortical bone fragility fractures by inhibiting osteoclastogenesis through noncanonical Jun-N-terminal kinase cascade [16]. Taken together, multiple Wnt ligands employing different signaling pathways have complex roles in regulating skeletal growth and bone metabolism.

We recently generated global and cell-specific Wnt1 knockout mouse models and demonstrated that mesenchymal cell derived-Wnt1 is a key regulator of bone metabolism affecting both trabecular and cortical compartments [17]. We also showed that Wnt1 functions in a juxtacrine manner, i.e. it requires cell-cell contact, to induce both osteoblast differentiation and activity as well as to suppress osteoclast differentiation. Similarly, Joeng and colleagues showed using Wnt1 loss- and gain-of-function mouse models that osteocyte-specific Wnt1 regulates osteoblast function during bone homeostasis [18]. Although very informative, the previous studies using mouse models with global or cell-specific Wnt1 knockout could not exclude the possibility that the effect of Wnt1 deletion on bone might due to early developmental effects.

To explore the role of Wnt1 in osteoblast lineage cells in adults, we

* Corresponding author at: Institute of Biomedicine, University of Turku, FI-20520 Turku, Finland.
E-mail address: riku.kiviranta@utu.fi (R. Kiviranta).

https://doi.org/10.1016/j.bone.2020.115754
Received 28 May 2020; Received in revised form 25 October 2020; Accepted 10 November 2020
Available online 13 November 2020

deleted Wnt1 using the tetracycline-controlled Osterix-Cre mouse line (Osx-Cre) and determined the effects of Wnt1 on bone formation in adult mice. As Wnt1 is an activator of Wnt/β-catenin signaling and deletion of Wnt1 in limb bud mesenchymal cells led to spontaneous fractures and severe osteopenia in mice, we hypothesized that Wnt1 knockout in osteoblast lineage would result in spontaneous fractures and bone loss in both trabecular and cortical bone. Moreover, we anticipated that inducible deletion of Wnt1 in adult mice would reduce bone mass in both trabecular and cortical bone. Thus, Wnt1 pathway could be targeted in the treatment of osteoporosis and other low bone mass pathologies.

2. Materials and methods

2.1. Generation of conditional $Wnt1^{-/-}_{Osx}$ knockout mice

To target *Wnt1* knockout to preosteoblasts, $Wnt1^{flox/+}$ female C57BL/6N mice were crossed with $Wnt1^{flox/+}$ male mice expressing Cre recombinase driven by the osterix (*Sp7*) promoter (B6.Cg-Tg(Sp7-tTA, tetO-EGFP/cre)1Amc/J) acquired from Jackson Laboratory (Supplementary Fig. 1A). The presence of the Osx-cre gene was determined using the following primer pair: forward primer (5′-CCAATTTACT-GACCGTACACC-3′) and reverse primer (5′- CCCGGCAAAA-CAGGTAGTTA-3′). 6–8 mice per genotype were used for analysis.

2.2. Regulation of Osx-Cre expression

To suppress Osx-Cre:GFP activity during fetal development, designated breeders received doxycycline (Dox) (Sigma-Aldrich) in their drinking water (0.2 mg/ml) during pregnancy until delivery. Lactating dams and $Wnt1^{-/-}_{Osx}$ offspring received Dox in their drinking water (1 mg/ml) until the age of 4 weeks (Fig. 2A, right). In the presence of Dox, tTA does not activate the transcription of GFP-Cre gene, keeping Wnt1 allele intact (Fig. 2A, left). Dox was then withdrawn to induce Wnt1 deletion and mice were analyzed at 8 and 12 weeks of age (Fig. 2A, right). Heterozygous mice (expressing both Osx-Cre and heterozygous floxed target gene) and Osx-Cre negative homozygous fl/fl littermates were used as controls. Animals (both males and females) were analyzed at the ages of 4 weeks, 8 weeks and 12 weeks. Mice were maintained in groups of up to 5 animals per cage and kept in a light-dark cycle of 12/12 h at room temperature in filter top cages. All mouse studies were approved by The Finnish Ethical Committee for experimental animals (Project license number: 5186/04.10.07/2017), and were in compliance with the international guidelines on the care and use of laboratory animals.

2.3. Microcomputed tomography analysis

Micro-CT (μCT) analyses on the tibias or femurs were performed using Skyscan 1272 μCT scanner (Skyscan, Kontich, Belgium) and an X-ray tube voltage of 70 kV and current of 142 μA, with a 0.5 mm aluminum filter. The scanning voxel resolution for tibia and femur was 8.37 μm and 5 μm, respectively. The scanning angular rotation was 192.8°, and the angular increment was 0.4°. Cross-sectional images were reconstructed with NRecon 1.4 software (Bruker micro-CT). For the analysis of the trabecular bone in tibia, a volumetric region of interest (ROI) excluding the cortical bone was defined at the metaphysis of the tibia starting 50 layers (418 μm) below the lower surface of the growth plate and extending 120 layers distally (1004 μm). For the analysis of cortical bone, a cylinder at the diaphysis of the tibia starting 400 layers (3348 μm) below the growth plate and extending for 100 layers (837 μm) was defined.

For the analysis of the trabecular bone in femur, a volumetric ROI was defined at the metaphysis of distal femur starting 120 layers (600 μm) above the surface of the distal growth plate and extending 240 layers proximally (1200 μm). For analysis of cortical bone, a cylinder at the diaphysis of the femur starting 1100 layers (5500 μm) above the growth plate and extending for 200 layers (1000 μm) was defined.

2.4. Bone histology and histomorphometry

Bone histomorphometry was performed as previously described [17]. In brief, mice were subcutaneously injected with calcein (20 mg/kg body weight) and demeclocycline (40 mg/kg body weight) (both from Sigma-Aldrich) 9 and 2 days prior to sacrifice for 12 and 8 week timepoints, respectively. The tibias were fixed in 4% formaldehyde overnight and dehydrated in 70% EtOH. The fixed bones were embedded in methyl methacrylate (Sigma-Aldrich, St.Louis, MO, USA). For analyses of trabecular bone, undecalcified 5 μm thick sections were cut with microtome, stained with Von Kossa method for mineralized bone, stained with 2% Toluidine Blue for the analysis of osteoblasts, osteoid and osteoclasts or stained with TRAP and counterstained with Toluidine Blue for confirming the analysis of osteoclasts. For analyses of cortical bone, the tibias were sectioned in the transverse plane with a diamond saw and unstained 100 μm-thick sections were analyzed for static and dynamic parameters, such as bone volume per tissue volume (BV/TV), cortical thickness (Cort.th), mineral apposition rate (MAR) and bone formation rate (BFR), respectively. All parameters were measured using the OsteoMeasure histomorphometry system (OsteoMetrics, USA) following the guideline of the American Society for Bone and Mineral Research (Dempster, 2013).

2.5. Quantitative real-time PCR

Immediately after the dissection, the humerus with bone marrow were snap-frozen in liquid nitrogen and then stored in −80 °C. The humeri were pulverized in liquid nitrogen and the RNA was isolated using TRIsure reagent (Bioline, Germany) followed by RNeasy Mini Kit (Qiagen, Germany). The cDNA was synthesized with SensiFAST cDNA Synthesis Kit (Bioline, Germany). RNA expression of the genes of interest was determined using Dynamo Flash SYBR Green qPCR Kit (ThermoFisher Scientific, Lithuania). Messenger RNA levels were normalized to β-actin expression by using $2^{-\Delta\Delta CT}$–method. Primer sequences for qPCR are provided in Supplementary Table 1.

2.6. Statistical analyses

The data were analyzed using GraphPad Prism software (GraphPad Software Inc.) and values are given as mean ± SD. For the comparisons of data following normal distribution, we performed 2-tailed Student's *t*-tests with a significance level of 0.05. For the comparisons of data that did not follow normal distribution, we performed Shapiro-Wilk test to detect normality among groups and applied the Mann-Whitney test for the comparisons between groups. One-way ANOVA with Bonferroni's comparisons test was used when comparing multiple groups to determine the statistical significance. $^{*}P < 0.05$, $^{**}P < 0.01$, $^{***}P < 0.001$, $^{****}P < 0.0001$.

3. Results

3.1. Deletion of Wnt1 in osteoblast lineage leads to spontaneous fractures and low bone mass

To assess to what extent the bone defects in Osx-Cre mice could affect the analysis of bone phenotypes in our Wnt1 conditional knockout mice and to decide which genotypes should be used as controls for further experiments, we first examined the skeleton of Osx-Cre Wnt1 conditional knockout mice without administration of doxycycline.

$Wnt1^{-/-}_{Osx}$ mice without doxycycline administration were viable but developed spontaneous fractures as early as 3 weeks of age (Fig. 1A). Fractures were mostly found in mid-tibia but also in humerus. Moreover, at 4 weeks of age, $Wnt1^{-/-}_{Osx}$ mice showed decreased body weight, as well

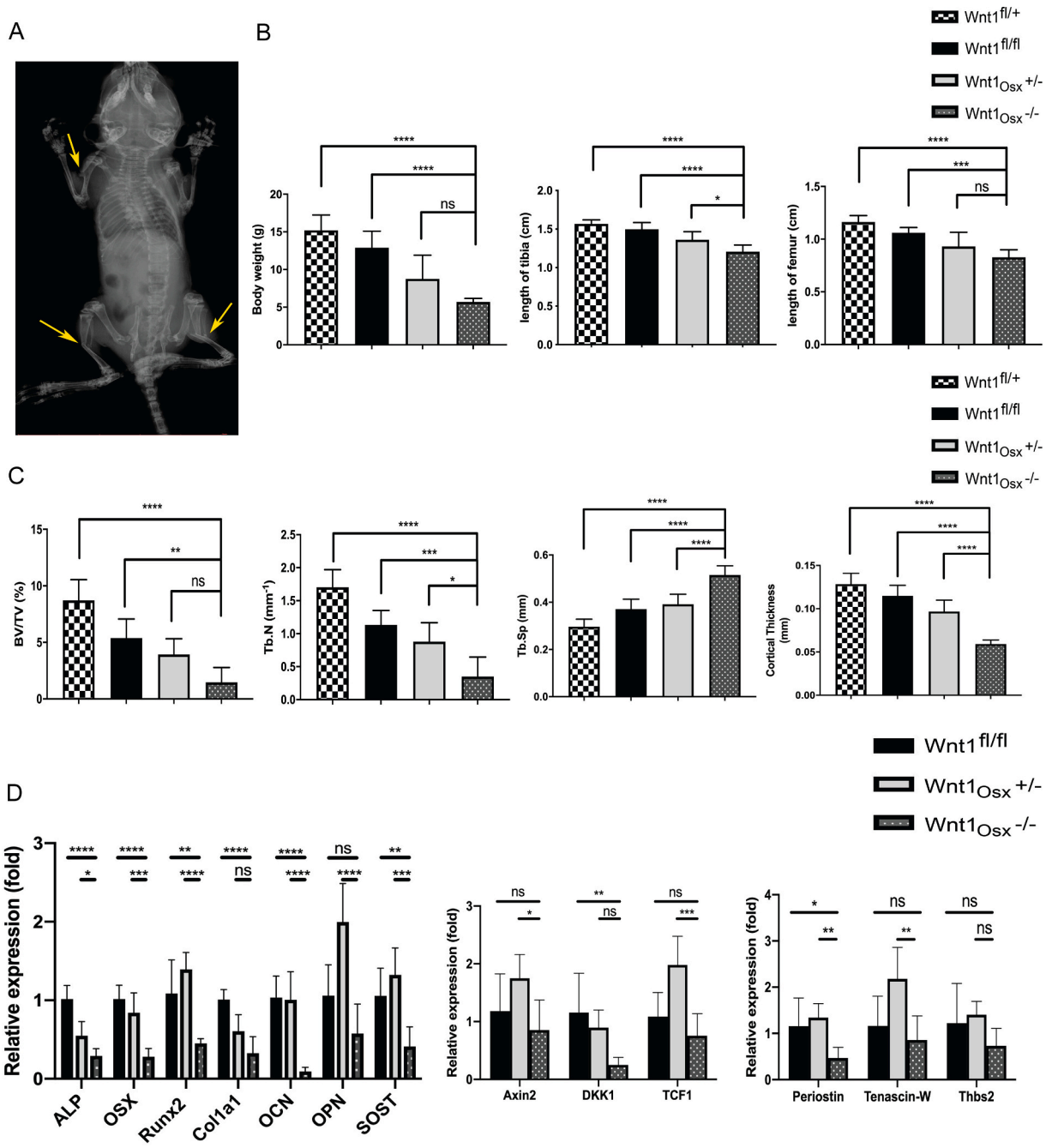

Fig. 1. Wnt1 deletion in osteoblast lineage leads to severe osteopenia and spontaneous fractures.
(A) Whole body X-ray image of 3 weeks old $Wnt1^{-/-}_{osx}$ mice. Fractures are indicated by yellow arrows. (B) Body weight and length of tibia and femur of 4-week-old $Wnt1^{fl/+}$, $Wnt1^{fl/fl}$, $Wnt1_{Osx}{}^{+/-}$ and $Wnt1_{Osx}{}^{-/-}$ male mice. ($n = 6$). (C) μCT analysis showing trabecular bone volume per tissue volume (BV/TV), trabecular number (Tb.N), trabecular separation (Tb.Sp) and cortical thickness in tibia of $Wnt1^{fl/+}$, $Wnt1^{fl/fl}$, $Wnt1_{Osx}{}^{+/-}$ and $Wnt1_{Osx}{}^{-/-}$ male mice at the age of 4 weeks in tibia. (n = 6). (D) mRNA expression levels of bone specific genes, Wnt signaling related genes and periosteal cell markers in humeri of $Wnt1^{fl/fl}$, $Wnt1_{Osx}{}^{+/-}$ and $Wnt1_{Osx}{}^{-/-}$ mice at the age of 4 weeks. (n = 6). Values are given as mean ± SD. *$P < 0.05$, **$P < 0.01$, ***$P < 0.001$, ****$P < 0.0001$ (One-way ANOVA). (For interpretation of the references to colour in this figure legend, the reader is referred to the web version of this article.)

as decreased length of tibia and femur compared to age-and gender-matched controls (Fig. 1B). Notably, the heterozygous knockout $Wnt1^{+/-}_{Osx}$ mice expressing both Osx-Cre and one functional Wnt1 allele were significantly lighter and their tibias and femurs were shorter than $Wnt1^{fl/fl}$ mice, confirming that the expression of the Osx-Cre transgene had an effect on body weight and tibia and femur length as has been previously described [19,20].

μCT analysis of tibia showed a 4-fold reduction in trabecular bone volume per tissue volume (BV/TV) with decreased trabecular number (Tb.N) and increased trabecular separation (Tb.Sp) in $Wnt1^{-/-}_{Osx}$ mice at 4 weeks of age (Fig. 1C). In addition, cortical bone thickness in $Wnt1^{-/-}_{Osx}$ mice was decreased by 50% compared to $Wnt1^{fl/fl}$ mice (Fig. 1C). Not surprisingly, heterozygous knockout $Wnt1^{+/-}_{Osx}$ mice displayed lower trabecular BV/TV, Tb.N, higher Tb.Sp and lower cortical thickness compared to the mice not expressing Osx-Cre ($Wnt1^{fl/fl}$) (Fig. 1C). As global $Wnt1^{+/-}$ mice present only a very modest bone phenotype, these data indicate that the Osx-Cre transgene itself has a small effect to the observed bone defects in $Wnt1^{-/-}_{Osx}$. Therefore, $Wnt1^{+/-}_{Osx}$ and $Wnt1^{fl/fl}$

were necessary controls for further experiments.

In line with the significantly decreased bone mass, the mRNA expression of markers for bone formation, such as alkaline phosphatase (ALP), osterix (OSX) and osteocalcin(OCN) were all downregulated in the bones of $Wnt1_{Osx}^{-/-}$ mice (Fig. 1D). When analyzing the mRNA expression of Wnt/β-catenin target genes, Dickkopf 1 (DKK1), which is a WNT signaling pathway inhibitor, Axin2 and transcription factor 1 (TCF1) were significantly downregulated (Fig. 1D). Furthermore, the mRNA expression of markers for periosteal cells, Periostin and Tenascin-W were downregulated in the bones of $Wnt1_{Osx}^{-/-}$ mice (Fig. 1D).

3.2. The deletion of Wnt1 in osteoblasts of adult mice causes a mild and transient osteopenia in metaphyseal trabecular bone

Based on our previously published data [17] and those presented here, Wnt1 deletion causes a severe developmental skeletal phenotype. To explore the function of Wnt1 in adult bone remodeling/modeling, we induced osteoblast-targeted Wnt1 knockout in adolescent mice by administration of Dox in drinking water until the age of 4 weeks.

Although by genotyping PCR a fade deletion band of Wnt1 was observed in the genomic DNA of 4-week-old $Wnt1_{Osx\text{-}Dox}^{-/-}$ mice ($Wnt1_{Osx}^{-/-}$ mice received Dox treatment until the age of 4 weeks) (Supplementary Fig. 1B), there was no difference in the body weights or bone lengths between $Wnt1_{Osx\text{-}Dox}^{-/-}$, $Wnt1_{Osx\text{-}Dox}^{+/-}$ and $Wnt1^{fl/fl}$ mice

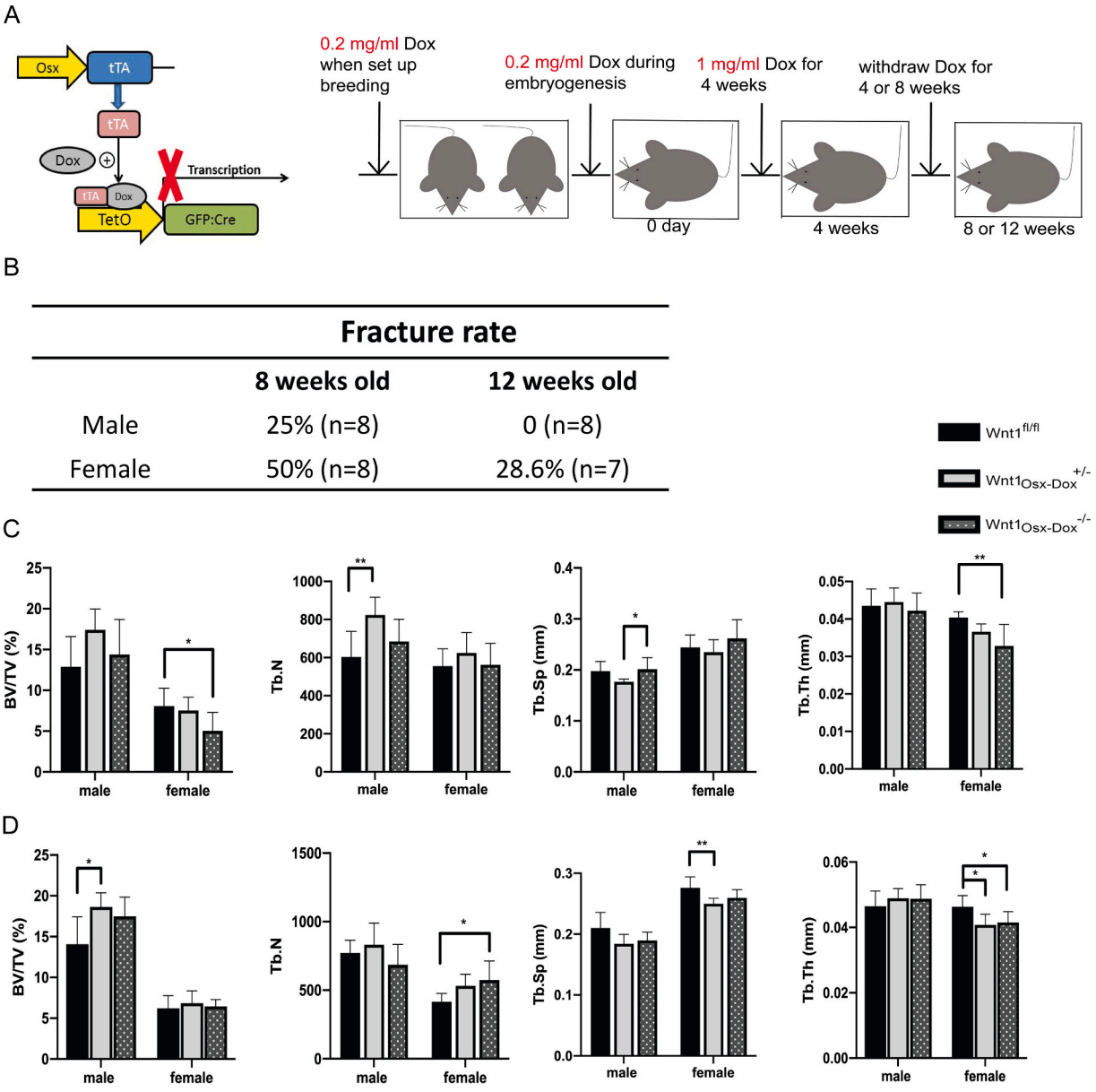

Fig. 2. The deletion of Wnt1 in osteoblasts of adult mice leads to modest and transient osteopenia in trabecular bone.
(A) Schematic view of Tet-off system used to generate the conditional knockout mice. The tTA driver is controlled by the *Osx* promoter gene to target the deletion of Wnt1 gene in osteoblast lineage. Wnt1 deletion is inhibited in the presence of Dox and induced when Dox is removed from the drinking water (left). A schematic presentation illustrating the experimental time points and duration of administration or withdrawal of Dox (right). (B) Fracture frequency of tibia presented as percentage of $Wnt1_{Osx\text{-}Dox}^{-/-}$ mice at 8 and 12 weeks of age, (4 weeks and 8 weeks after Dox removal, respectively), starting from the age of 4 weeks. The data were evaluated by X-ray. (C, D) μCT analysis showing trabecular bone volume per tissue volume (BV/TV), trabecular number (Tb.N), trabecular separation (Tb.Sp) and trabecular thickness (Tb. Th) in distal femur of $Wnt1^{fl/fl}$, $Wnt1_{Osx\text{-}Dox}^{+/-}$ and $Wnt1_{Osx\text{-}Dox}^{-/-}$ mouse of both male and female mice at 8 (C) and 12 (D) weeks of age. ($n = 8$). Values are given as mean ± SD. *$P < 0.05$, **$P < 0.01$, ***$P < 0.001$, ****$P < 0.0001$ (One-way ANOVA).

(Supplementary Fig. 2 A and B). However, the body weight and bone length was significantly increased in 4-week-old $Wnt1^{-/-}_{Osx\text{-}Dox}$ mice under Dox treatment compared to the gender and age-matched $Wnt1^{-/-}_{Osx}$ mice without Dox treatment (Supplementary Fig. 2 A and B). In addition, spontaneous fractures were not observed in long bones in $Wnt1^{-/-}_{Osx\text{-}Dox}$ mice under Dox treatment (Supplementary Fig. 2C). These data indicated that even though the dose of Dox cannot completely suppress the expression of GFP-Cre fusion protein, the inducible Wnt1 deletion mouse model is still appropriate for studying Wnt1 function in adult mice. As expected, Wnt1 deletion was observed in bone after removing Dox from drinking water for 4 and 8 weeks (8 and 12 weeks of age, respectively) (Supplementary Fig. 1C).

$Wnt1^{-/-}_{Osx\text{-}Dox}$ mice developed normally and their body weights did not differ from the littermate controls at 8 or 12 weeks of age (data not shown). However, diaphyseal fractures were observed in the tibias of $Wnt1^{-/-}_{Osx\text{-}Dox}$ mice. The penetrance of the fractures was 25% in male and 50% in female at 8 weeks of age (4 weeks after deletion of Wnt1) (Fig. 2B). At 12 weeks, male mice did not exhibit spontaneous fractures in tibia, while 29% of females displayed tibia fractures at 12 weeks of age (8 weeks after deletion of Wnt1) (Fig. 2B). μCT analysis of the distal femur of female $Wnt1^{-/-}_{Osx\text{-}Dox}$ mice revealed a mild trabecular osteopenia with 37.7% and 33.1% reduction in BV/TV at 8 weeks of age compared to $Wnt1^{fl/fl}$ and $Wnt1^{+/-}_{Osx\text{-}Dox}$ control mice, respectively (Fig. 2C). The trabecular thickness (Tb.Th) was also reduced by 18.6% in female 8-week-old $Wnt1^{-/-}_{Osx\text{-}Dox}$ mice compared to $Wnt1^{fl/fl}$ control mice, while the reduction was not significant when compared to $Wnt1^{+/-}_{Osx\text{-}Dox}$ control mice (Fig. 2C). No significant differences were observed in trabecular bone parameters in 8-week-old male $Wnt1^{-/-}_{Osx\text{-}Dox}$ mice when compared to $Wnt1^{fl/fl}$ control mice (Fig. 2C). However, when compared to $Wnt1^{+/-}_{Osx\text{-}Dox}$ control mice, the trabecular number (Tb.N) was reduced by 17% while trabecular separation (Tb.Sp) was increased by 13.3% in $Wnt1^{-/-}_{Osx\text{-}Dox}$ male mice (Fig. 2C). At the age of 12 weeks, the trabecular bone parameters were unchanged in $Wnt1^{-/-}_{Osx\text{-}Dox}$ and control male mice (Fig. 2D).

Histomorphometric analyses of proximal tibia confirmed that there was no significant structural bone phenotype or alterations in cellular or dynamic parameters in female or male $Wnt1^{-/-}_{Osx\text{-}Dox}$ mice at 12 weeks of age (Table 1 and data not shown). Taken together, Wnt1 deletion in osteoblasts of adult mice led to mild osteopenia in younger females, but did not affect trabecular bone structure in younger males or older females or males.

Table 1
Trabecular bone characteristics analyzed by histomorphometry in the proximal tibia of 12-week-old female $Wnt1^{+/-}_{Osx\text{-}Dox}$ and $Wnt1^{-/-}_{Osx\text{-}Dox}$ mice after removing Dox for 8 weeks, starting from the age of 4 weeks.

	$Wnt1^{+/-}_{Osx\text{-}Dox}$ (n = 7)	$Wnt1^{-/-}_{Osx\text{-}Dox}$ (n = 7)
Bone volume/tissue volume (BV/TV; %)	8.16 ± 2.95	8.00 ± 2.74
Trabecular thickness (Tb.Th; μm)	39.91 ± 8.80	40.85 ± 5.50
Trabecular number (Tb.N; /mm)	2.01 ± 0.38	1.92 ± 0.48
Trabecular separation (Tb.Sp; μm)	478.15 ± 102.82	530.31 ± 186.47
Mineral apposition rate (MAR; μm/day)	1.83 ± 1.04	2.24 ± 0.51
Mineralizing surface/bone surface (MS/BS; %)	27.35 ± 8.45	29.30 ± 10.05
Bone formation rate (BFR; mm^3/mm^2/year)	0.55 ± 0.30	0.68 ± 0.31
Osteoblast surface/bone surface (Ob.S/BS; %)	4.69 ± 3.01	4.58 ± 2.94
Osteoblast number/bone perimeter (N.Ob/B.Pm; /mm)	3.70 ± 2.06	3.45 ± 1.54
Osteoclast surface/bone surface (Oc.S/BS; %)	7.50 ± 3.52	7.79 ± 2.34
Osteoclast number/bone perimeter (N.Oc/B.Pm; /mm)	3.31 ± 1.59	3.14 ± 0.75
Eroded surface/bone surface (ES/BS; %)	4.99 ± 2.35	4.35 ± 0.94

Values are given as mean ± SD. student's t-test.

3.3. The deletion of Wnt1 in osteoblasts of adult mice leads to reduced cortical bone thickness

As diaphyseal fractures in $Wnt1^{-/-}_{Osx\text{-}Dox}$ mice were frequently observed, we next evaluated whether the Wnt1 deletion in osteoblasts affected cortical bone thickness in the long bones of adult mice. As expected, the deletion of Wnt1 in long bone genomic DNA was more strongly induced at 8 weeks after removing Dox than at 4 weeks (Supplementary Fig. 1C). μCT analysis of proximal femur showed reduced BV/TV and cortical thickness (Cort.Th) in 8-week old female but not in male $Wnt1^{-/-}_{Osx\text{-}Dox}$ mice 4 weeks after Dox removal compared to $Wnt1^{fl/fl}$ or $Wnt1^{+/-}_{Osx\text{-}Dox}$ control mice (Fig. 3A and B). A significant reduction of cortical thickness was observed in femur of both genders in 12-week old $Wnt1^{-/-}_{Osx\text{-}Dox}$ mice at 8 weeks after Dox removal (Fig. 3C). These findings suggest that Wnt1 specifically controls maintenance of cortical bone homeostasis in adult skeleton. In addition, although cortical bone phenotype was observed in both male and female mice, it was generally more pronounced in females compared to males (e.g. in 12-week-old mice femur cortical thickness was decreased by 15% in females and by 8.1% in males when compared to $Wnt1^{fl/fl}$ control mice.)

Moreover, $Wnt1^{-/-}_{Osx\text{-}Dox}$ mice displayed a trend for decreased total tissue volume (TV) and significantly lower cortical bone volume in both 8 and 12-week-old mice compared to control mice, while the volume of bone marrow (BMV) was unchanged (Fig. 3C and Table 2). These data suggest that slower periosteal apposition could contribute to the thinner cortical bone in $Wnt1^{-/-}_{Osx\text{-}Dox}$ mice.

When analyzing the mRNA expression of Wnt/β-catenin target genes, Axin2 and DKK1 were significantly downregulated in the bones of $Wnt1^{-/-}_{Osx\text{-}Dox}$ mice compared to $Wnt1^{+/-}_{Osx\text{-}Dox}$ mice (Fig. 3D). However, the mRNA expression of markers for the periosteal cells were unchanged (Fig. 3D).

3.4. Wnt1 regulates periosteal bone formation in adult mice

To investigate the mechanisms of Wnt1 deletion on the reduced cortical bone thickness, we performed dynamic histomorphometric analyses of the distal tibiae of female mice. Histomorphometric data confirmed a reduced cortical thickness (−10.1%, $P < 0.05$) in 12-week-old female $Wnt1^{-/-}_{Osx\text{-}Dox}$ mice when compared with $Wnt1^{+/-}_{Osx\text{-}Dox}$ (Fig. 4A). Fluorescent images of distal tibia cross-sections showed that the fluorochrome labels were more abundant in periosteal bone of $Wnt1^{+/-}_{Osx\text{-}Dox}$ mice compared to $Wnt1^{-/-}_{Osx\text{-}Dox}$ mice. The double labels were absent more frequently in periosteal bone of $Wnt1^{-/-}_{Osx\text{-}Dox}$ mice, while in endosteal side, the fluorochrome labels were visible in both genotypes, although the signal was much stronger in $Wnt1^{+/-}_{Osx\text{-}Dox}$ mice compared to $Wnt1^{-/-}_{Osx\text{-}Dox}$ mice (Fig. 4B). Histomorphometric analysis indicated a notable reduction in periosteal bone formation rate per bone volume (BFR/BV; −98.7%, $P < 0.01$) in $Wnt1^{-/-}_{Osx\text{-}Dox}$ mice female mice (Fig. 4B) that was mainly due to reduced mineralizing bone surface (MS/BS; −82%, $P < 0.01$) and mineral apposition rate (MAR; −94%, $P < 0.05$) (Fig. 4B). In contrast, at the endosteal surface, mineralized bone surface and bone formation were unaffected in $Wnt1^{-/-}_{Osx\text{-}Dox}$ mice (Fig. 4C, Table 3). To test whether this could be due to defect in osteocytes, we measured osteocyte number in the proximal tibias and mRNA expression of osteocyte markers (DMP1 and SOST) in humeral bones of 12-weeks-old mice. No significant differences were detected in either osteocyte number or the expression of osteocyte marker genes between $Wnt1^{+/-}_{Osx\text{-}Dox}$ and $Wnt1^{-/-}_{Osx\text{-}Dox}$ mice (data not shown). These data demonstrate that the reduced cortical bone thickness observed in $Wnt1^{-/-}_{Osx\text{-}Dox}$ mice is due to impaired periosteal bone formation.

4. Discussion

Osteoporosis characterized by low bone mass and increased bone fragility represents a major disease burden in our aging population. We have recently reported that Wnt1 deletion in limb bud mesenchymal

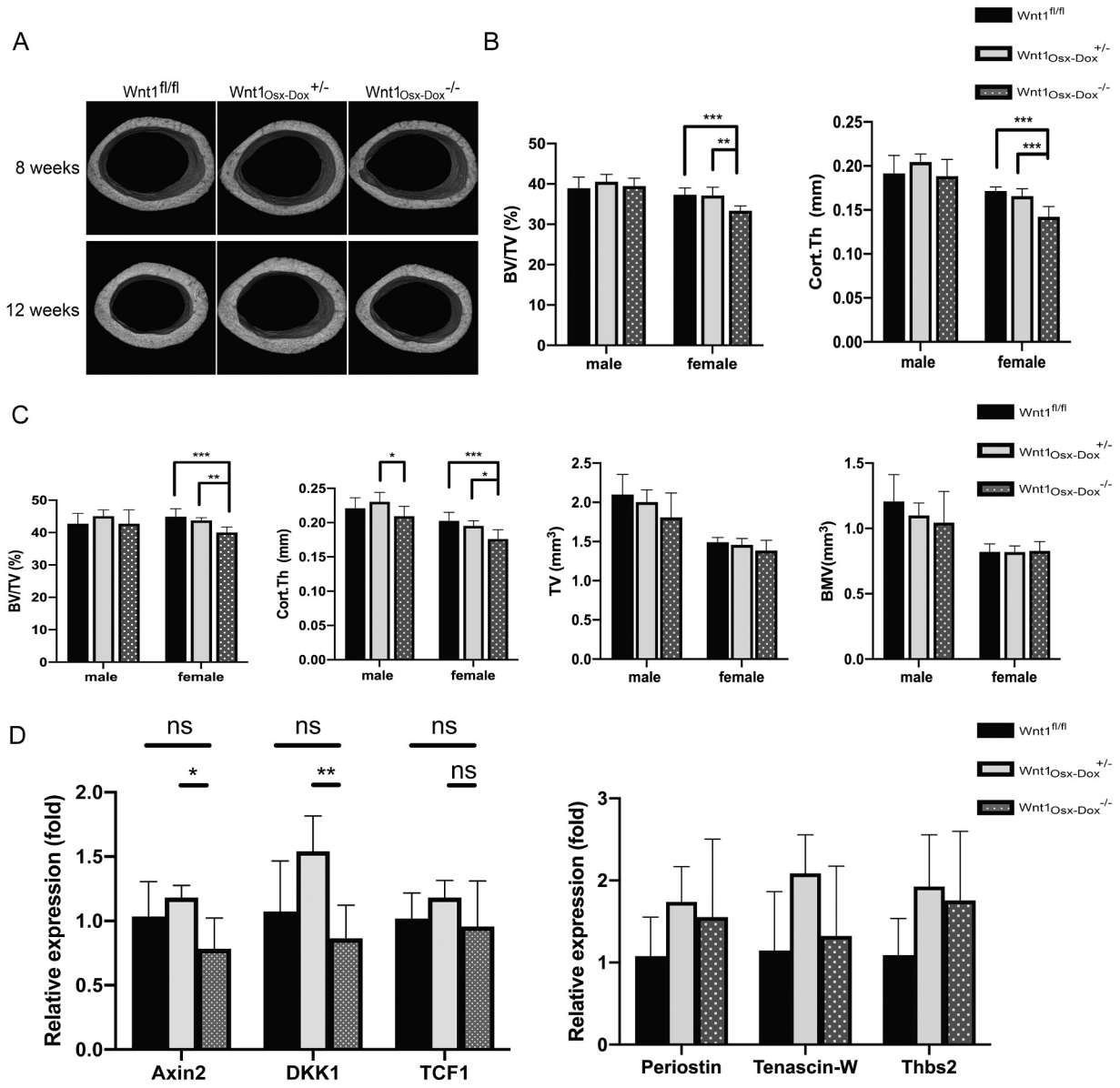

Fig. 3. The deletion of Wnt1 in osteoblasts of adult mice reduces cortical bone thickness.
(A) μCT images of cortical bone in the proximal femur of a $Wnt1^{fl/fl}$, $Wnt1^{+/-}_{Osx\text{-}Dox}$ and $Wnt1^{-/-}_{Osx\text{-}Dox}$ mouse at 8 and 12 weeks of age. (B) μCT analysis showing cortical bone volume per tissue volume (BV/TV) and cortical thickness (Cort.Th) in the proximal femur of $Wnt1^{fl/fl}$, $Wnt1^{+/-}_{Osx\text{-}Dox}$ and $Wnt1_{Osx\text{-}Dox}{}^{-/-}$ mice at 8 weeks of age. ($n = 8$). (C) μCT analysis showing BV/TV, cortical thickness, tissue volume (TV) and bone marrow volume (BMV) in the proximal femur of $Wnt1^{fl/fl}$, $Wnt1^{+/-}_{Osx\text{-}Dox}$ and $Wnt1_{Osx\text{-}Dox}{}^{-/-}$ mice at 12 weeks of age. (D) mRNA expression levels of Wnt signaling related genes and periosteal cell markers in humeri of $Wnt1^{fl/fl}$, $Wnt1_{Osx\text{-}Dox}{}^{+/-}$ and $Wnt1_{Osx\text{-}Dox}{}^{-/-}$ mice at the age of 12 weeks. ($n = 6$). Values are given as mean ± SD. $^{*}P < 0.05$, $^{**}P < 0.01$, $^{***}P < 0.001$, $^{****}P < 0.0001$ (One-way ANOVA).

cells in a mouse model results in osteopenia and spontaneous fractures, suggesting that Wnt1 is a key regulator of bone metabolism affecting both trabecular and cortical compartments. However, these studies could not exclude the possibility that the effect of Wnt1 deletion on bone might be caused by early developmental effects. Therefore, it was necessary to investigate the role of Wnt1 in adult skeleton. For this purpose we generated an inducible Wnt1 deletion mouse model and demonstrate here that Wnt1 is an important regulator of periosteal, modeling based bone formation in adult mice.

In the present study, we generated an osteoblast-lineage specific Wnt1 knockout mouse model using tetracycline-controlled Osx-Cre mouse line. Osx-Cre mice are commonly used to target osteoblasts; they carry both tTA under the regulation of *Osterix* (*Sp7*) promoter and a tetracycline responsive element-controlled GFP-Cre fusion protein. In this system, treatment with tetracycline analog doxycycline (Dox) prevents the expression of GFP-Cre fusion protein and the recombination of target gene. This system can be used for cell type and time point specific gene targeting. However, skeletal defects have been observed in Osx-Cre transgenic mice, including delayed calvaria ossification, fracture calluses at multiple skeletal sites and hypomineralization in coronal sutural area [19–21]. In our current study, we observed abnormal growth of teeth in $Wnt1^{+/-}_{Osx}$ mice, expressing both Osx-Cre and heterozygous floxed Wnt1 gene. Feeding with soft food did not rescue the significantly decreased body weight of $Wnt1^{+/-}_{Osx}$ mice compared to Osx-Cre-negative control ($Wnt1^{fl/+}$) (Fig. 1B). In addition, we found that Osx-Cre transgene itself had distinct effects on both trabecular and cortical bone parameters. Therefore, it is of great importance to include both floxed and Cre transgenic littermate controls in Osx-Cre mediated conditional

Table 2
Cortical bone characteristics of proximal femur of $Wnt1^{fl/fl}$, $Wnt1^{+/-}_{Osx\text{-}Dox}$ and $Wnt1^{-/-}_{Osx\text{-}Dox}$ mice.

	$Wnt1^{fl/fl}$	$Wnt1^{+/-}_{Osx\text{-}Dox}$	$Wnt1^{-/-}_{Osx\text{-}Dox}$
8-week-old male mice	**n = 8**	**n = 8**	**n = 8**
Tissue volume(TV; mm^3)	1.8 ± 0.4	1.9 ± 0.2	1.7 ± 0.2
Bone volume (BV; mm^3)	0.7 ± 0.2	0.8 ± 0.1	0.7 ± 0.1
Bone marrow volume (BMV; mm^3)	1.1 ± 0.3	1.1 ± 0.2	1.0 ± 0.2
Total porosity (Po; %)	6.3 ± 1.1	7.2 ± 2.7	7.4 ± 1.7
8-week-old female mice	***n* = 8**	**n = 8**	**n = 8**
Tissue volume(TV; mm^3)	1.5 ± 0.1	1.4 ± 0.1	$1.2 \pm 0.2^{\#\#,*}$
Bone volume (BV; mm^3)	0.6 ± 0.0	0.5 ± 0.0	$0.4 \pm 0.1^{\#\#\#\#,**}$
Bone marrow volume (BMV; mm^3)	1.0 ± 0.1	0.9 ± 0.1	$0.8 \pm 0.2^{\#}$
Total porosity (Po; %)	6.8 ± 1.5	7.1 ± 1.9	7.0 ± 3.5
12-week-old male mice	**n = 7**	**n = 7**	**n = 8**
Tissue volume(TV; mm^3)	2.1 ± 0.3	2.0 ± 0.3	1.8 ± 0.3
Bone volume (BV; mm^3)	0.9 ± 0.1	0.9 ± 0.1	0.8 ± 0.1
Bone marrow volume (BMV; mm^3)	1.2 ± 0.2	1.1 ± 0.1	1.0 ± 0.2
Total porosity (Po; %)	3.7 ± 0.6	2.8 ± 0.5	3.7 ± 0.8*
12-week-old female mice	**n = 8**	**n = 8**	**n = 7**
Tissue volume(TV; mm^3)	1.5 ± 0.1	1.5 ± 0.1	1.4 ± 0.1
Bone volume (BV; mm^3)	0.67 ± 0.04	0.64 ± 0.04	$0.56 \pm 0.07^{\#\#,*}$
Bone marrow volume (BMV; mm^3)	0.8 ± 0.1	0.8 ± 0.0	0.8 ± 0.1
Total porosity (Po; %)	3.9 ± 0.6	4.2 ± 1.1	3.7 ± 0.9

Cortical bone μCT analyses of proximal femur in 8-week-old and 12-week-old $Wnt1^{fl/fl}$, $Wnt1^{+/-}_{Osx\text{-}Dox}$ and $Wnt1^{-/-}_{Osx\text{-}Dox}$ males and females 4 weeks and 8 weeks after Dox removal, starting from the age of 4 weeks. Values are given as mean ± SD. $^{\#}P < 0.05$, $^{\#\#}P < 0.01$, $^{\#\#\#}P < 0.001$, $^{\#\#\#\#}P < 0.0001$ compared to $Wnt1^{fl/fl}$ mice. *P < 0.05, **P < 0.01, ***P < 0.001, ****P < 0.0001 compared to $Wnt1^{+/-}_{Osx\text{-}Dox}$ mice. (One-way ANOVA).

knockout mice studies to ensure accurate interpretation of any observed bone phenotypes.

The mice were subcutaneously injected with calcein and demeclocycline to label bone formation for histomorphometric analysis before sacrificing. Both doxycycline and demeclocycline belong to the same tetracycline family. Therefore, oral administration of doxycycline in mouse will cause fluorescent background in bone tissue, resulting in difficulty to identify the demeclocycline label. In order to minimize the effects of Dox, the dose of Dox should not be too high, but sufficient enough to suppress the deletion of Wnt1. In our study, we found that there was slight leakage of Cre recombinase resulting in mild deletion of Wnt1 in long bone (Supplementary Fig. 1B). However, Dox treatment in knockout mice efficiently rescued the loss of body weight, tooth malocclusion and suppressed the spontaneous fractures in long bone (Supplementary Fig. 2A and B). Moreover, the fluorescent background in bone tissue caused by Dox did not affect histomorphometric analysis. These data indicated that the inducible Osx-Cre – Wnt1 deletion mouse model using Dox administration was applicable to our research questions.

Mutations in WNT1 in humans result in early-onset osteoporosis and osteogenesis imperfecta (OI), while deletion of Wnt1 in mice leads to severe developmental bone phenotype with fractures [5–8,17,18,22]. These data demonstrate the essential role for Wnt1 in skeletal development and growth. Although previous studies have been very informative, the possibility that the effect of Wnt1 on the skeleton might be caused by early developmental effects could not be excluded. Using the novel mouse model generated in the present study, it was possible to investigate the role of Wnt1 in regulating bone homeostasis in adult skeleton. We clearly demonstrated that Wnt1 is crucial for cortical bone but not for trabecular bone homeostasis in adult mice. In addition, although we observed that Wnt1 deletion in adult mice caused reduced cortical bone thickness in both males and females, it was generally more

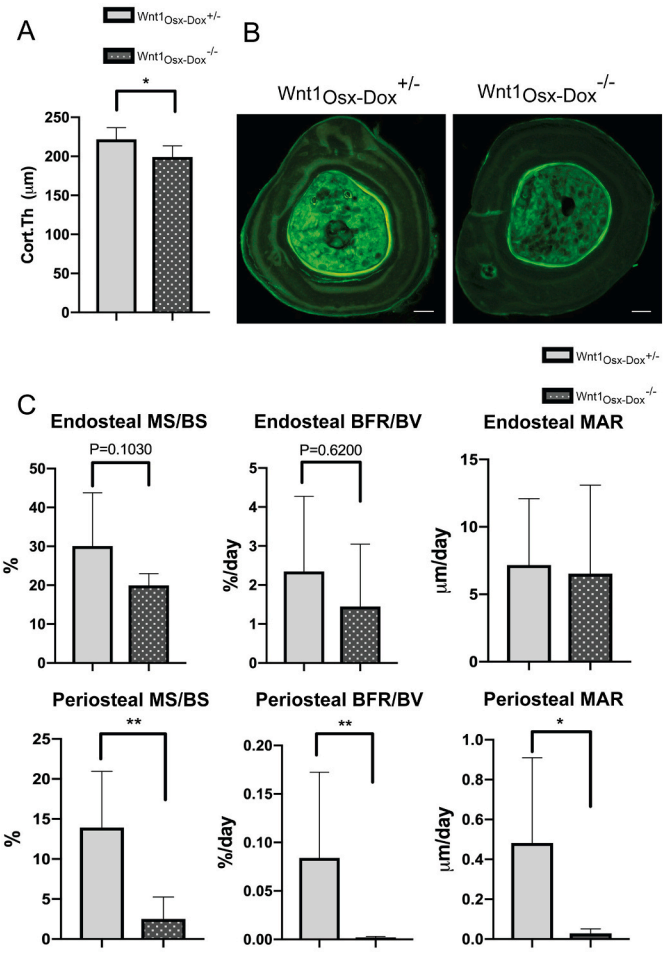

Fig. 4. Wnt1 regulates periosteal bone formation in adult female mice. (A) Cortical thickness of distal tibia of female $Wnt1_{Osx\text{-}Dox}{}^{+/-}$ and $Wnt1_{Osx\text{-}Dox}{}^{-/-}$ mice at 12 weeks of age measured by histomorphometry (n = 6). (B) Fluorescent images of cross-sections of distal tibia of female $Wnt1_{Osx\text{-}Dox}{}^{+/-}$ and $Wnt1_{Osx\text{-}Dox}{}^{-/-}$ mice at 12 weeks of age. Scale bar corresponds to 100 μm. (C) Histomorphometry of 12-week-old female $Wnt1_{Osx\text{-}Dox}{}^{+/-}$ and $Wnt1_{Osx\text{-}Dox}{}^{-/-}$ mice showing endosteal and periosteal mineralizing surface per bone surface (MS/BS), bone formation rate per bone volume (BFR/BV) and mineral apposition rate (MAR) (n = 6). Values are given as mean ± SD. *P < 0.05, **P < 0.01, ***P < 0.001. (Mann-Whitney test).

Table 3
Cortical bone characteristics of distal tibia of 12-week-old female $Wnt1^{+/-}_{Osx\text{-}Dox}$ and $Wnt1^{-/-}_{Osx\text{-}Dox}$ mice after removing Dox for 8 weeks.

	$Wnt1^{+/-}_{Osx\text{-}Dox}$ (n = 7)	$Wnt1^{-/-}_{Osx\text{-}Dox}$ (n = 7)
Total tissue area (T.Ar; mm^2)	1.56 ± 0.12	1.37 ± 0.25
Total bone area (B.Ar; mm^2)	0.50 ± 0.03	0.46 ± 0.05
Cortical bone volume per tissue volume (BV/TV; %)	32.08 ± 2.33	34.26 ± 4.53
Periosteal bone formation rate (BFR/BS; mm^3/mm^2/day)	0.09 ± 0.09	0.001 ± 0.002**
Endocortical bone formation rate (BFR/BS; mm^3/mm^2/day)	2.60 ± 2.07	1.43 ± 1.58

Histomorphometric analyses of distal tibia cortical bone of 12-week-old female $Wnt1^{+/-}_{Osx\text{-}Dox}$ and $Wnt1^{-/-}_{Osx\text{-}Dox}$ mice 8 weeks after Dox removal, starting from the age of 4 weeks. Data are reported as mean ± SD. $Wnt1^{-/-}_{Osx\text{-}Dox}$ vs $Wnt1^{+/-}_{Osx\text{-}Dox}$ control mice. *P < 0.05, **P < 0.01, ***P < 0.001. (Mann-Whitney test).

pronounced in females compared to males. This could be due to the stimulatory effect of androgens on the periosteal bone growth in the male mice that could partially compensate for the loss of Wnt1 [23]. Further investigations are required to reveal the molecular mechanisms behind the sexual dimorphism found in $Wnt1^{-/-}_{Osx\text{-}Dox}$ mice.

The reduced cortical bone thickness in the adult Wnt1 deficient mice was due to decreased periosteal bone formation, while the endosteal bone formation was unaffected, as demonstrated by the histomorphometric analyses. Wnt1 deletion led to reductions in both mineralized bone surface and mineral apposition rate, suggesting that both lower number of periosteal cells and lower bone forming activity per cell contributed to the phenotype. In contrast to cortical bone formation, trabecular bone formation and bone resorption were unchanged in $Wnt1^{-/-}_{Osx\text{-}Dox}$ (Table 1), indicating that Wnt1 mainly regulates modeling-based bone formation in adult mice. Sclerostin, encoded by the SOST gene, is an osteocyte-derived negative regulator of bone formation [24,25]. It is an inhibitor of WNT signaling by binding to the low-density lipoprotein receptor-related protein 5/6 (Lrp5/6) [26–28]. Sclerostin binds to the loop 1 of the Lrp5/6 receptor where it inhibits the binding of Wnt1-type Wnt ligands to the receptor [29]. Interestingly, inhibition of sclerostin by anti-sclerostin antibody romosozumab predominantly stimulates modeling-based bone formation at both trabecular and cortical surface [30]. In addition, Joeng and colleagues recently demonstrated that romosozumab treatment partially rescued the bone phenotype of Wnt1 mutation-carrying Swaying mouse model [18]. Taken together, our work and those of others suggest that inhibition of sclerostin by romosozumab stimulates modeling-based bone formation at least in part by allowing for Wnt1 binding to the Lrp5/6 receptor. Thus romosozumab is an intriguing treatment option for patients with Wnt1-related osteoporosis to enhance periosteal bone formation at cortical bone sites.

Our data also illustrates the complexity of Wnt signaling in bone with multiple receptors, inhibitors and numerous Wnt ligands each with specific and redundant functions. Movérare-Skrtic et al. previously showed that osteoblast-derived Wnt16 protects cortical bone by suppressing osteoclastogenesis and subsequently cortical bone resorption [16]. Osteoblast-derived Wnt5a in turn induces osteoclastogenesis via ROR2 receptor mediated in non-canonical Wnt signaling in osteoclast progenitor cells. We previously showed that Wnt1 does suppress osteoclastogenesis in trabecular bone in young adult mice in vivo and does this by direct cell-cell contact via canonical Wnt signaling pathway [17]. However, we did not observe increased bone resorption in either trabecular or cortical compartments in the adult $Wnt1^{-/-}_{Osx\text{-}Dox}$ mice, suggesting that Wnt1 regulates trabecular bone turnover during rapid growth but periosteal bone formation in adult mice.

5. Conclusions

We present here compelling evidence that osteoblastic Wnt1 is a key regulator of cortical bone thickness in adult mice. Wnt1 improves cortical thickness in adult mice by stimulating modeling-based bone formation. These data identify Wnt1 signaling as a target for the development of novel treatment strategies to enhance periosteal bone formation and cortical bone strength to achieve better protection especially against non-vertebral fractures.

Funding

This study was funded by the Academy of Finland (R.K.: 298625, 268535, 139165), Novo Nordisk Foundation, Sigrid Juselius Foundation, the Finnish Cultural Foundation, Orion Research Foundation and the work at TCDM by funding provided by the University of Turku and Biocenter Finland.

CRediT authorship contribution statement

R.K. conceived the idea for the study. R.K., F.W. designed the experiments. F.W. and P.R. collected mouse samples. F.W. and P.R. performed the experiments. F.W., P.R. and R.K. analyzed the data. R.K. and T.J.H. supervised the work and R.K. acquired the funding. F.W. drafted the manuscript. F.W., T.J.H. and R.K. edited the manuscript and all authors accepted the final version of the manuscript.

Declaration of competing interest

The authors declare no conflict of interests.

Acknowledgements

The authors thank Merja Lakkisto, Dr. Fuping Zhang and the staff of Turku Central Animal Laboratory for their excellent technical assistance.

Appendix A. Supplementary data

Supplementary data to this article can be found online at https://doi.org/10.1016/j.bone.2020.115754.

References

[1] J.E. Compston, M.R. McClung, W.D. Leslie, Osteoporosis, Lancet, 2019, https://doi.org/10.1016/S0140-6736(18)32112-3.
[2] T.D. Rachner, S. Khosla, L.C. Hofbauer, Osteoporosis: now and the future, Lancet (2011), https://doi.org/10.1016/S0140-6736(10)62349-5.
[3] R. Baron, F. Gori, Targeting WNT signaling in the treatment of osteoporosis, Curr. Opin. Pharmacol. (2018), https://doi.org/10.1016/j.coph.2018.04.011.
[4] K. Maeda, Y. Kobayashi, M. Koide, S. Uehara, M. Okamoto, A. Ishihara, T. Kayama, M. Saito, K. Marumo, The regulation of bone metabolism and disordersby wnt signaling, Int. J. Mol. Sci. (2019), https://doi.org/10.3390/ijms20225525.
[5] S.M. Pyott, T.T. Tran, D.F. Leistritz, M.G. Pepin, N.J. Mendelsohn, R.T. Temme, B. A. Fernandez, S.M. Elsayed, E. Elsobky, I. Verma, S. Nair, E.H. Turner, J.D. Smith, G.P. Jarvik, P.H. Byers, WNT1 mutations in families affected by moderately severe and progressive recessive osteogenesis imperfecta, Am. J. Hum. Genet. 92 (2013) 590–597, https://doi.org/10.1016/j.ajhg.2013.02.009.
[6] C.M. Laine, K.S. Joeng, P.M. Campeau, R. Kiviranta, K. Tarkkonen, M. Grover, J. T. Lu, M. Pekkinen, M. Wessman, T.J. Heino, V. Nieminen-Pihala, M. Aronen, T. Laine, H. Kröger, W.G. Cole, A.-E. Lehesjoki, L. Nevarez, D. Krakow, C.J. R. Curry, D.H. Cohn, R.A. Gibbs, B.H. Lee, O. Mäkitie, WNT1 mutations in early-onset osteoporosis and osteogenesis imperfecta, N. Engl. J. Med. 368 (2013) 1809–1816, https://doi.org/10.1056/NEJMoa1215458.
[7] K. Keupp, F. Beleggia, H. Kayserili, A.M. Barnes, M. Steiner, O. Semler, B. Fischer, G. Yigit, C.Y. Janda, J. Becker, S. Breer, U. Altunoglu, J. Grünhagen, P. Krawitz, J. Hecht, T. Schinke, E. Makareeva, E. Lausch, T. Cankaya, J.A. Caparrós-Martín, P. Lapunzina, S. Temtamy, M. Aglan, B. Zabel, P. Eysel, F. Koerber, S. Leikin, K. C. Garcia, C. Netzer, E. Schönau, V.L. Ruiz-Perez, S. Mundlos, M. Amling, U. Kornak, J. Marini, B. Wollnik, Mutations in WNT1 cause different forms of bone fragility, Am. J. Hum. Genet. 92 (2013) 565–574, https://doi.org/10.1016/j.ajhg.2013.02.010.
[8] S. Fahiminiya, J. Majewski, J. Mort, P. Moffatt, F.H. Glorieux, F. Rauch, Mutations in WNT1 are a cause of osteogenesis imperfecta, J. Med. Genet. 50 (2013) 345–348, https://doi.org/10.1136/jmedgenet-2013-101567.
[9] S. Niemann, C. Zhao, F. Pascu, U. Stahl, U. Aulepp, L. Niswander, J.L. Weber, U. Müller, Homozygous WNT3 mutation causes tetra-Amelia in a large consanguineous family, Am. J. Hum. Genet. (2004), https://doi.org/10.1086/382196.
[10] C.G. Woods, S. Stricker, P. Seemann, R. Stern, J. Cox, E. Sherridan, E. Roberts, K. Springell, S. Scott, G. Karbani, S.M. Sharif, C. Toomes, J. Bond, D. Kumar, L. Al-Gazali, S. Mundlos, Mutations in WNT7A cause a range of limb malformations, including fuhrmann syndrome and Al-Awadi/Raas-Rothschild/Schinzel phocomelia syndrome, Am. J. Hum. Genet. (2006), https://doi.org/10.1086/506332.
[11] P.N. Kantaputra, S. Mundlos, W. Sripathomsawat, A novel homozygous Arg222Trp missense mutation in WNT7A in two sisters with severe Al-Awadi/Raas-Rothschild/Schinzel phocomelia syndrome, Am. J. Med. Genet. Part A. (2010), https://doi.org/10.1002/ajmg.a.33673.
[12] M.B. Mutlu, A. Cetinkaya, N. Koc, G. Ceylaner, B. Erguner, H. Aydın, S. Karaman, O. Demirci, K. Goksu, A. Karaman, A novel missense mutation, p.(R102W) in WNT7A causes Al-Awadi Raas-Rothschild syndrome in a fetus, Eur. J. Med. Genet. (2016), https://doi.org/10.1016/j.ejmg.2016.09.009.
[13] P.N. Kantaputra, S. Kapoor, P. Verma, M. Kaewgahya, K. Kawasaki, A. Ohazama, J. R. Ketudat Cairns, Al-Awadi-Raas-Rothschild syndrome with dental anomalies and

a novel WNT7A mutation, Eur. J. Med. Genet. (2017), https://doi.org/10.1016/j.ejmg.2017.09.005.
[14] B. Wang, T. Sinha, K. Jiao, R. Serra, J. Wang, Disruption of PCP signaling causes limb morphogenesis and skeletal defects and may underlie Robinow syndrome and brachydactyly type B, Hum. Mol. Genet. (2011), https://doi.org/10.1093/hmg/ddq462.
[15] K. Maeda, Y. Kobayashi, N. Udagawa, S. Uehara, A. Ishihara, T. Mizoguchi, Y. Kikuchi, I. Takada, S. Kato, S. Kani, M. Nishita, K. Marumo, T.J. Martin, Y. Minami, N. Takahashi, Wnt5a-Ror2 signaling between osteoblast-lineage cells and osteoclast precursors enhances osteoclastogenesis, Nat. Med. (2012), https://doi.org/10.1038/nm.2653.
[16] S. Movérare-Skrtic, P. Henning, X. Liu, K. Nagano, H. Saito, A.E. Börjesson, K. Sjögren, S.H. Windahl, H. Farman, B. Kindlund, C. Engdahl, A. Koskela, F. P. Zhang, E.E. Eriksson, F. Zaman, A. Hammarstedt, H. Isaksson, M. Bally, A. Kassem, C. Lindholm, O. Sandberg, P. Aspenberg, L. Sävendahl, J.Q. Feng, J. Tuckermann, J. Tuukkanen, M. Poutanen, R. Baron, U.H. Lerner, F. Gori, C. Ohlsson, Osteoblast-derived WNT16 represses osteoclastogenesis and prevents cortical bone fragility fractures, Nat. Med. (2014), https://doi.org/10.1038/nm.3654.
[17] F. Wang, K. Tarkkonen, V. Nieminen-Pihala, K. Nagano, R. Al Majidi, T. Puolakkainen, P. Rummukainen, J. Lehto, A. Roivainen, F.P. Zhang, O. Mäkitie, R. Baron, R. Kiviranta, Mesenchymal cell-derived Juxtacrine Wnt1 signaling regulates osteoblast activity and osteoclast differentiation, J. Bone Miner. Res. (2019), https://doi.org/10.1002/jbmr.3680.
[18] K.S. Joeng, Y.C. Lee, J. Lim, Y. Chen, M.M. Jiang, E. Munivez, C. Ambrose, B. H. Lee, Osteocyte-specific WNT1 regulates osteoblast function during bone homeostasis, J. Clin. Invest. 127 (2017) 2678–2688, https://doi.org/10.1172/JCI92617.
[19] L. Wang, Y. Mishina, F. Liu, Osterix-Cre transgene causes craniofacial bone development defect, Calcif. Tissue Int. (2015), https://doi.org/10.1007/s00223-014-9945-5.
[20] R.A. Davey, M.V. Clarke, S. Sastra, J.P. Skinner, C. Chiang, P.H. Anderson, J. D. Zajac, Decreased Body Weight in Young Osterix-Cre Transgenic Mice Results in Delayed Cortical Bone Expansion and Accrual, Transgenic Res, 2012, https://doi.org/10.1007/s11248-011-9581-z.
[21] W. Huang, B.R. Olsen, Skeletal Defects in Osterix-Cre Transgenic Mice, Transgenic Res, 2015, https://doi.org/10.1007/s11248-014-9828-6.
[22] J. Luther, T.A. Yorgan, T. Rolvien, L. Ulsamer, T. Koehne, N. Liao, D. Keller, N. Vollersen, S. Teufel, M. Neven, S. Peters, M. Schweizer, A. Trumpp, S. Rosigkeit, E. Bockamp, S. Mundlos, U. Kornak, R. Oheim, M. Amling, T. Schinke, J.P. David, Wnt1 is an Lrp5-independent bone-anabolic Wnt ligand, Sci. Transl. Med. (2018), https://doi.org/10.1126/scitranslmed.aau7137.
[23] D. Vanderschueren, L. Vandenput, S. Boonen, M.K. Lindberg, R. Bouillon, C. Ohlsson, Androgens and bone, Endocr. Rev. (2004), https://doi.org/10.1210/er.2003-0003.
[24] R. Baron, M. Kneissel, WNT signaling in bone homeostasis and disease: from human mutations to treatments, Nat. Med. (2013), https://doi.org/10.1038/nm.3074.
[25] J. Delgado-Calle, A.Y. Sato, T. Bellido, Role and Mechanism of Action of Sclerostin in Bone, Bone, 2017, https://doi.org/10.1016/j.bone.2016.10.007.
[26] M. Semënov, K. Tamai, X. He, SOST is a ligand for LRP5/LRP6 and a Wnt signaling inhibitor, J. Biol. Chem. (2005), https://doi.org/10.1074/jbc.M504308200.
[27] X. Li, Y. Zhang, H. Kang, W. Liu, P. Liu, J. Zhang, S.E. Harris, D. Wu, Sclerostin binds to LRP5/6 and antagonizes canonical Wnt signaling, J. Biol. Chem. (2005), https://doi.org/10.1074/jbc.M413274200.
[28] D.L. Ellies, B. Viviano, J. McCarthy, J.P. Rey, N. Itasaki, S. Saunders, R. Krumlauf, Bone density ligand, sclerostin, directly interacts with LRP5 but not LRP5G171V to modulate Wnt activity, J. Bone Miner. Res. (2006), https://doi.org/10.1359/jbmr.060810.
[29] M.K. Chang, I. Kramer, H. Keller, J.H. Gooi, C. Collett, D. Jenkins, S.A. Ettenberg, F. Cong, C. Halleux, M. Kneissel, Reversing LRP5-dependent osteoporosis and SOST deficiency-induced sclerosing bone disorders by altering WNT signaling activity, J. Bone Miner. Res. (2014), https://doi.org/10.1002/jbmr.2059.
[30] M.S. Ominsky, Q.T. Niu, C. Li, X. Li, H.Z. Ke, Tissue-level mechanisms responsible for the increase in bone formation and bone volume by sclerostin antibody, J. Bone Miner. Res. (2014), https://doi.org/10.1002/jbmr.2152.